frontiers | Frontiers in Chemistry

ORIGINAL RESEARCH
published: 27 April 2022
doi: 10.3389/fchem.2022.892090

Effects of the Urease Concentration and Calcium Source on Enzyme-Induced Carbonate Precipitation for Lead Remediation

Lin Wang[1,2], *Wen-Chieh Cheng*[1,2]*, *Zhong-Fei Xue*[1,2] *and Wenle Hu*[1,2]

[1]School of Civil Engineering, Xi'an University of Architecture and Technology, Xi'an, China, [2]Shaanxi Key Laboratory of Geotechnical and Underground Space Engineering (XAUAT), Xi'an, China

Heavy metal contamination during the rapid urbanization process in recent decades has notably impacted our fragile environments and threatens human health. However, traditional remediation approaches are considered time-consuming and costly, and the effect sometimes does not meet the requirements expected. The present study conducted test tube experiments to reproduce enzyme-induced carbonate precipitation applied to lead remediation under the effects of urease concentration and a calcium source. Furthermore, the speciation and sequence of the carbonate precipitation were simulated using the Visual MINTEQ software package. The results indicated that higher urease concentrations can assure the availability of CO_3^{2-} during the enzyme-induced carbonate precipitation (EICP) process toward benefiting carbonate precipitation. The calcium source determines the speciation of carbonate precipitation and subsequently the Pb remediation efficiency. The use of CaO results in the dissolution of $Pb(OH)_2$ and, therefore, discharges Pb ions, causing some difficulty in forming the multi-layer structure of carbonate precipitation and degrading Pb remediation. The findings of this study are useful in widening the horizon of applications of the enzyme-induced carbonate precipitation technology to heavy metal remediation.

Keywords: urease enzyme, carbonate precipitation, heavy metal, urease concentration, calcium source

Edited by:
Florent Allais,
AgroParisTech Institut des Sciences et Industries du Vivant et de L'environnement, France

Reviewed by:
Isaac Ahenkorah,
University of South Australia, Australia
Wei Li,
Nanjing University, China

***Correspondence:**
Wen-Chieh Cheng
w-c.cheng@xauat.edu.cn

Specialty section:
This article was submitted to Green and Sustainable Chemistry, a section of the journal Frontiers in Chemistry

Received: *08 March 2022*
Accepted: *25 March 2022*
Published: *27 April 2022*

Citation:
Wang L, Cheng W-C, Xue Z-F and Hu W (2022) Effects of the Urease Concentration and Calcium Source on Enzyme-Induced Carbonate Precipitation for Lead Remediation. Front. Chem. 10:892090. doi: 10.3389/fchem.2022.892090

INTRODUCTION

Heavy metal contamination in the soil and underground water seriously threatens surrounding fragile environments and human health (Kim et al., 2001; Mohan et al., 2006; Bai et al., 2017; Chang et al., 2019; Chen et al., 2022a; Hu et al., 2020; Bai et al., 2021; Hu et al., 2021; Liu et al., 2021; Xue et al., 2021; Hu et al., 2022; Wang et al., 2022). Such heavy metal contamination remediation by the traditional soil flushing measure is deemed time-consuming and costly since heavy metal ions are easily adsorbed by soil particles, and intensive industrial activities further aggravate heavy metal contamination (Yang et al., 2014; An et al., 2019; Kumar and Dwivedi, 2019; Bai et al., 2021; Cheng et al., 2021; Duan et al., 2021; Wei et al., 2021; Yuan et al., 2021; Chen et al., 2022b). In the past few years, various remediation measures, including but not limited to physical, chemical, and biological measures, have been proposed to deal with heavy-metal contamination (Dhami et al., 2013; Shashank et al., 2016; Qian et al., 2017; Rahman et al., 2020; Ahenkorah et al., 2021a; Hu et al., 2021; Jiang et al., 2021; and Xue et al., 2022). Amongst the heavy metal contamination remediation measures, enzyme-induced carbonate precipitation (EICP) is an environmentally friendly, efficient, and sustainable measure. Recently, the EICP technology has been widely applied to calcareous sand reinforcement (Ahenkorah et al., 2021b; Chen et al., 2021; Cui et al., 2021; and Meng et al., 2021), while studies on the remediation of contaminations, including organic and inorganic contaminants using the EICP technology, are remarkably limited (Neupane et al., 2013; Putra et al., 2016; and Moghal et al., 2020a). During the EICP process, urease catalyzes urea hydrolysis toward producing CO_3^{2-}. The obtained CO_3^{2-} precipitates with a calcium source, resulting in carbonate precipitation (Fisher et al., 2017; and Sun et al., 2021). **Eqs 1–4** show the biochemical reactions involving urea hydrolysis driven by urease in the EICP process (Mobley and Hausinger, 1989; Fujita et al., 2010; Achal et al., 2012; Achal et al., 2013; Mitchelf et al., 2013; Mugwar and Harbottle, 2016).

$$CO(NH_2)_2 + H_2O \rightarrow 2NH_3 + CO_2, \tag{1}$$

$$2NH_3 + 2H_2O \leftrightarrow 2NH_4^+ + 2OH^-, \tag{2}$$

$$CO_2 + 2OH^- \leftrightarrow HCO_3^- + OH^- \leftrightarrow CO_3^{2-} + H_2O, \tag{3}$$

$$Ca^{2+} + CO_3^{2-} \rightarrow CaCO_3 \downarrow. \tag{4}$$

A significant body of research conducted over the last few years has greatly enhanced our understanding of improving the mechanical properties of soil and mitigating dust emissions using the EICP technology. Yuan et al. (2020) studied an improved EICP method by adding organic materials (i.e., skim milk powder and brown sugar) into the urease solution and demonstrated its improvement in the mechanical properties of fine-grained soils. Almajed et al. (2018) conducted a baseline study to evaluate the effect of urease solution components on the precipitated efficiency, and a threshold of the carbonate fraction was further identified through a series of unconfined compression tests. Hamdan and Kavazanjian, (2016) performed wind tunnel tests, and the mitigation of fugitive dust emissions was attained by carbonate precipitation using the EICP technology. Hoang et al., (2019) examined the shearing resistance in sand and silt-sand mixtures using the carbonate precipitation catalyzed by the urease enzyme extracted from plants. These results demonstrate an exciting potential for the use of the EICP technology to achieve soil reinforcement and mitigation of dust emissions.

Recently, it is also attempted as a remediation measure for immobilizing organic and inorganic contaminants. Moghal et al., 2020b evaluated the efficiency of EICP in restricting the migration of heavy metals by using ethylenediaminetetraacetic acid (EDTA) and citric acid as extractants. The results indicated that the retention efficiency of the remediated soil can be improved by 30% in comparison with the unremediated soil. Nam et al. (2016) examined the ability of the *Canavalia ensiformis* extract to catalyze urea to form carbonate precipitation on heavy metals resulting from abandoned mines and employed X-ray diffraction and scanning electron microscopy (SEM) to confirm the precipitation speciation. The findings of this work suggested that such an extract is effective in immobilizing heavy metals and preventing their diffusion into surrounding environments. Although there are limited studies on the immobilization of heavy metals by the EICP approach, higher concentrations of contaminants (i.e., > than 5 mmol/L in solution or 400 mg/kg in soil) have been neglected (Li et al., 2015; Kang and So, 2016; Zhu et al., 2017). The Pb contamination sites correspond to approximately 20% in all heavy metal–contaminated sites in mainland China, while the highest Pb concentration measured near a smelter in the Fujian province was up to 30,430 mg/kg (Duan et al., 2016). Therefore, an efficient, economical measure to remediate the heavy metal–contaminated sites is of great necessity to protect fragile environments. However, commercial and bacteria-derived sources of the urease enzyme are either expensive or cumbersome (Nafisi et al., 2019; Wu et al., 2020). The objectives of this study are as follows: 1) to investigate the effects of the urease concentration and calcium source on the enzyme-induced carbonate precipitation for high concentration Pb remediation through a series of preliminary test tube experiments using the plant-derived urease enzyme as the catalyst and 2) to identify the speciation and sequence of carbonate precipitation using Visual MINTEQ simulations toward revealing the mechanisms affecting the Pb remediation efficiency.

MATERIALS AND METHODS

Urease Enzyme Extraction

Canavalia ensiformis was used in this study to prepare the urease enzyme using simple, economical extraction processes, including crushing, sieving, primary centrifugation, and secondary centrifugation (Yuan et al., 2020). The details are as follows: 1) *Canavalia ensiformis* was crushed using the plant grinding machine, thereby sieving with a mesh sieve (apertures = 0.15 mm); 2) the jack bean and ethanol solution were mixed in a ratio of 1:10 (g: ml), and the mixture solution was centrifuged for 30 min and then stored in the refrigerator for 4 h; 3) after that, the solution was centrifuged again for 1 h, and the precipitation of secondary centrifugation was the urease used in this study. It should be noted that the urease enzyme should be stored in a refrigerator at −20°C prior to its use. The urease enzyme is suggested to be used within 24 h after it is derived.

Urease Activity Tests

At standard conditions (30°C), 1 international unit (IU) of the enzyme activity is the amount of 1.0 μmol catalyzed transformation in 1 min (Mobley and Hausinger, 1989). Furthermore, a modified measure, proposed by Van Paassen (2011), was also used to enhance the accuracy of urease activity measurements. For the test, 1 ml of urease solution was mixed with 9 ml 1.11 mol/L urea, with electrical conductivity (EC), measured at 5, 10, and 15 min after mixing at room temperature. The modified measure can be expressed as follows:

$$\text{Urease activity} = \frac{EC_5 + EC_{10} + EC_{15}}{15} \times 10 \times 11.11\,(\text{mmol urea min}^{-1}), \tag{5}$$

where EC_5, EC_{10}, and EC_{15} are electrical conductivities at 5, 10, and 15 min, respectively. The modified electrical conductivity method yielded the urease activity being 99.8 mM Urea min-1, while the Nessler's reagent colorimetric method yielded a urease activity of 342.7 U/g. The former reflects the amount of urea hydrolyzed per minute. However, the latter reflects the required amount of enzyme converting 1 μM of the substrate using a specialized unit U/g. For this reason, the two values are not found on the same basis, although the Nessler's reagent colorimetric method adopted in the present work can describe the urease activity in a more straightforward manner. On the other hand, the NH_4^+ concentration was measured *via* a combination of the Nessler's reagent and spectrophotometer, which aims to describe the degree of urea hydrolysis.

Test Tube Experiments

The effects of urease concentration and the calcium source on Pb remediation were investigated through a series of test tube experiments. Three urease concentrations (3 g/L, 6 g/L, and 9 g/L) and three calcium sources ($CaCl_2$, $Ca(CH_3COO)_2$, and CaO) were adopted in the test tube experiments. The calcium source concentration used in the test tube experiments is 0.25 mol/L, while the urea concentration is 0.5 mol/L. Lead contaminant ($Pb(NO_3)_2$) concentrations adopted include both the low and high ranges, namely, 5 mmol/L, 10 mmol/L, 30 mmol/L, 40 mmol/L, and 50 mmol/L. The solution applied to the test tube experiments consisted of distilled water, urea, $Pb(NO_3)_2$, $CaCl_2$, and the urease enzyme. The preparation of the solution is depicted in **Supplementary Figure S1**. Catalyzing urea hydrolysis was handled at an indoor temperature of about 26°C and was conducted for a 48-h period, following inoculation. The measurements of pH, NH_4^+ concentration, and remaining Pb^{2+} concentration were conducted after 48 h. It is widely accepted that NH_4^+ and OH^- are the products of urea hydrolysis using the EICP technology, and they determine whether comprehensive urea hydrolysis is attained. The degree of urea hydrolysis not only dominates the amount of carbonate precipitation but also reflects the remaining Pb^{2+} concentration and remediation efficiency. The more the Pb^{2+} precipitated with the carbonate, the lesser will be the remaining Pb^{2+} and the higher the remediation efficiency. Prior to the measurement of the NH_4^+ concentration, the mixed solution was centrifuged and acidified to a pH lower than 2.0 for the sake of NH_4^+ measurement. Furthermore, the mixed solution was diluted 100–500 times, allowing the measurement to be undertaken. It was worth noting that all the precipitations were separated from the solution through the vacuum filtration method at the end of the tests and dried at 30°C for 3 days before being subjected to mass measurement (Keykha et al., 2018). All aforementioned tests had three biological replicates with coefficient of variance (COV) < 10%.

Visual MINTEQ Simulation

Given that the test tube experiments are not capable of providing the speciation and sequence of carbonate precipitation, it was simulated using the Visual MINTEQ software package. Here, urea hydrolysis was modeled as the initial condition about NH_4^+ and CO_3^{2-} with a stoichiometric ratio of 2:1 (Gat et al., 2017). The simulation for the evolution of the precipitation speciation was determined by the degrees of urea hydrolysis that require the inputs of NH_4^+ and CO_3^{2-} concentrations toward differentiating the abiotic precipitation from the biotic precipitation that directly plays roles in urea hydrolysis (Xue et al., 2022).

RESULTS

Relationship of Urease Concentration versus Lead Remediation Efficiency

It is widely accepted that ammonium (NH_4^+) and hydroxide (OH^-) ions are the products of urea hydrolysis using the EICP technology (**Eqs 1–3**), and therefore, the NH_4^+ concentration and pH are considered appropriate in determining whether comprehensive urea hydrolysis is attained. Its measurements were conducted during the EICP process. The variations of NH_4^+ concentration and pH when subjected to no urease and urease at concentrations ranging from 3 g/L to 9 g/L are shown in **Figures 1A,B**. Prior to introducing urease, the pH is always lower than 6 and appears insensitive to the concentration of $Pb(NO_3)_2$. However, the pH increases and surpasses 6 while catalyzing urea hydrolysis using the urease enzyme. Furthermore, the pH is generally increased with the increase of the urease concentration, and for urease at 3 g/L, there is a decrease when subjected to $Pb(NO_3)_2$ at 30 mmol/L (see **Figure 1A**). On the other hand, the urease is also on the way to catalyze urea hydrolysis toward producing NH_4^+ (see **Figure 1B**). Furthermore, the NH_4^+ concentration is generally decreased with the increase of the $Pb(NO_3)_2$ concentration. A significant drop in the $Pb(NO_3)_2$ concentration is also present when $Pb(NO_3)_2$ is at 30 mmol/L. Such a drop is not significant when subjected to higher urease concentrations (e.g. > 3 g/L). The variations of the measured precipitation mass when subjected to urease at 3 g/L, 6 g/L, and 9 g/L are shown in **Figure 1C**. It is clear that the precipitation mass is increased with the increase of the urease concentration and its maximum being 0.14 g, resulting from the urease at 9 g/L, presents when the $Pb(NO_3)_2$ concentration is at 50 mmol/L. Furthermore, the produced precipitation mass is generally increased with the increase of the $Pb(NO_3)_2$ concentration.

To assess the effectiveness of Pb remediation, a remediation efficiency defined as a ratio of the remaining Pb^{2+} concentration to the initial Pb^{2+} concentration was used in the present study. The lower the remaining Pb^{2+} concentration, the higher is the Pb^{2+} remediation efficiency. The variations of the remaining Pb^{2+} concentration and Pb remediation efficiency when subjected to urease at 3 g/L, 6 g/L, and 9 g/L, respectively, are shown in **Figure 1D**. The relationship of the remaining Pb^{2+} concentration versus $Pb(NO_3)_2$ concentration for the urease at 3 g/L lies above that for the urease at 6 g/L which is underlaid by that for the urease at 9 g/L. These results show that the higher the urease concentration, the lower is the remaining Pb^{2+} concentration. By measuring the remaining Pb ion concentration, the remediation efficiency against different urease concentrations is measured to be higher than 99.5%. Its maximum presents when the urease is at 9 g/L and reaches approximately 100%.

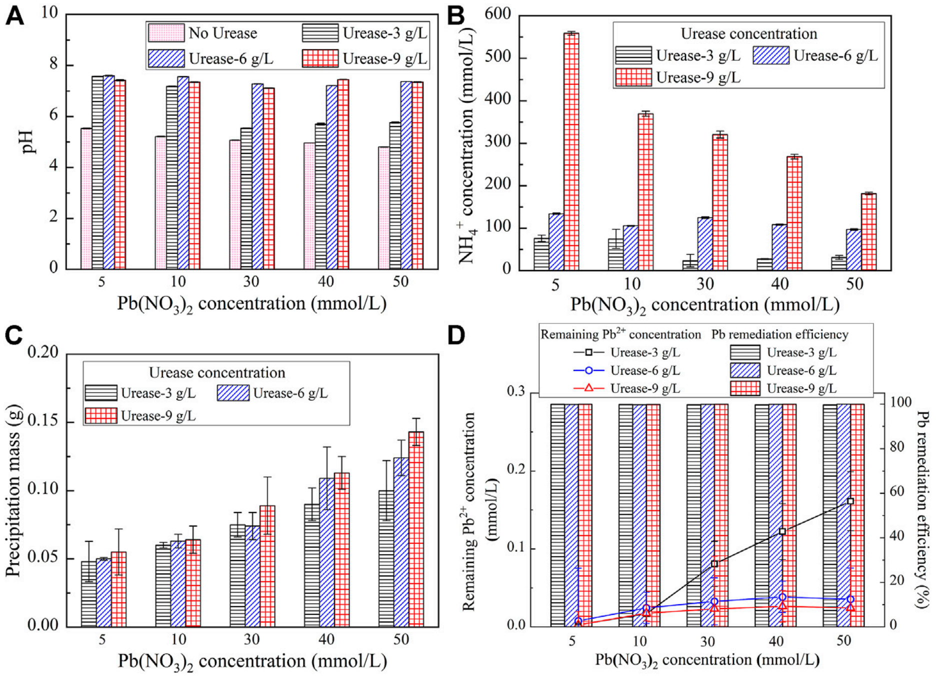

FIGURE 1 | (A) Relationship of pH versus $Pb(NO_3)_2$ concentration; **(B)** Relationship of the NH_4^+ concentration versus $Pb(NO_3)_2$ concentration; **(C)** Relationship of the precipitation mass versus $Pb(NO_3)_2$ concentration; and **(D)** Relationship of the Pb^{2+} concentration and Pb remediation efficiency versus $Pb(NO_3)_2$ concentration.

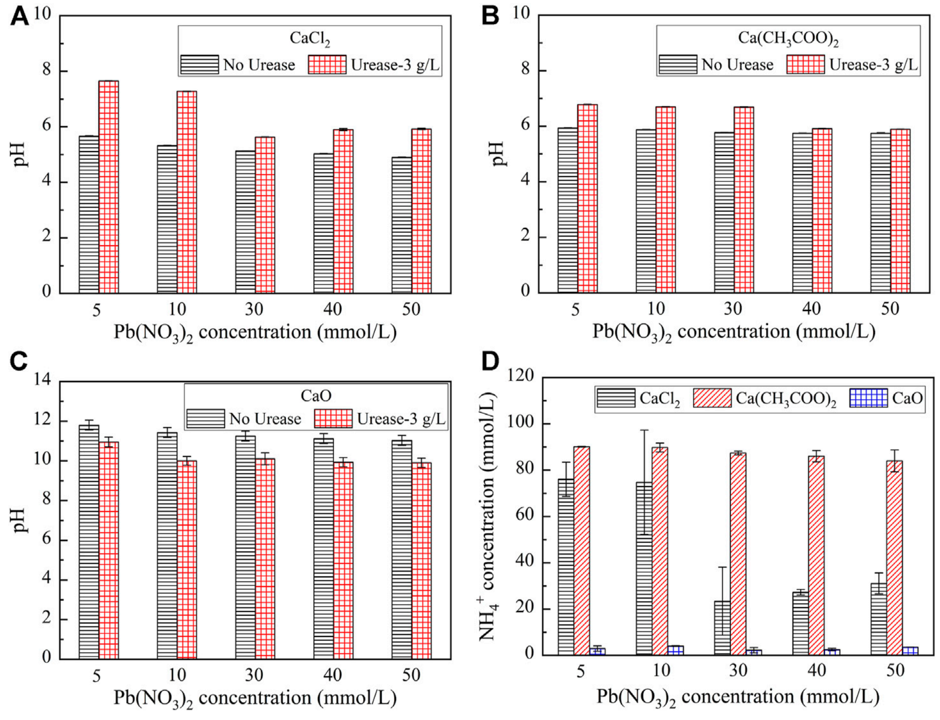

FIGURE 2 | Relationship of pH and NH_4^+ concentrations versus the $Pb(NO_3)_2$ concentration considering different calcium sources: **(A)** $CaCl_2$; **(B)** $Ca(CH_3COO)_2$; **(C)** CaO; and **(D)** Relationship of the NH_4^+ concentration versus $Pb(NO_3)_2$ concentration.

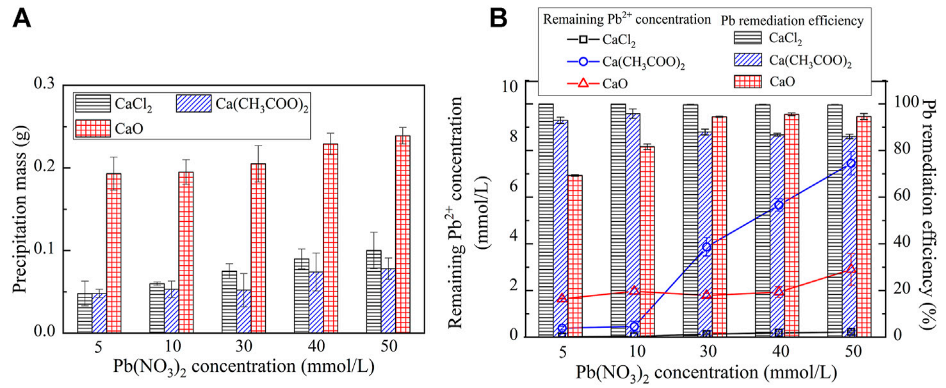

FIGURE 3 | (A) Relationship of the precipitation mass versus $Pb(NO_3)_2$ concentration and **(B)** Relationship of the Pb^{2+} concentration and remediation efficiency versus $Pb(NO_3)_2$ concentration.

Relationship of Calcium Source Versus Lead Remediation Efficiency

Given that the effect of the calcium source is considered crucial in improving Pb remediation, three calcium sources, including calcium chloride ($CaCl_2$), calcium acetate ($Ca(CH_3COO)_2$), and calcium oxide (CaO), were taken into account in the test tube experiments. Despite the Pb remediation efficiency being approximately 100% at 9 g/L, an efficiency being higher than 99.5% was derived at 3 g/L. The efficiency of 3 g/L was, therefore, adopted in the following analysis for the sake of economy. The variations of pH and NH_4^+ concentrations when subjected to $CaCl_2$, $Ca(CH_3COO)_2$, and CaO are shown in **Figure 2**. The pH, while catalyzing urea hydrolysis using urease, is always in excess of that prior to the urea hydrolysis except the case of calcium oxide (see **Figures 2A–C**). Furthermore, the pH is decreased with the increase of the $Pb(NO_3)_2$ concentration. Moreover, for the same $Pb(NO_3)_2$ concentration, the NH_4^+ concentration is the highest when subjected to $Ca(CH_3COO)_2$ (see **Figure 2D**). The NH_4^+ concentration is the lowest when subjected to CaO.

The variations of the measured carbonate precipitation mass when subjected to $CaCl_2$, $Ca(CH_3COO)_2$, and CaO are shown in **Figure 3A**. The results indicate that the carbonate precipitation mass, when subjected to CaO, is much greater than that subjected to $CaCl_2$ and $Ca(CH_3COO)_2$, and its maximum reaches 0.23 g. Furthermore, the precipitation mass is generally increased with the increase in the $Pb(NO_3)_2$ concentration. The variations of the remaining Pb^{2+} concentration and Pb remediation efficiency, when subjected to $CaCl_2$, $Ca(CH_3COO)_2$, and CaO, are shown in **Figure 3B**. The relationship of the remaining Pb^{2+} concentration versus $Pb(NO_3)_2$ concentration, when subjected to $Ca(CH_3COO)_2$ and CaO, lies above that subjected to $CaCl_2$. The Pb remediation efficiency, when subjected to different calcium sources, performs very well and is generally in excess of 70%. The best remediation efficiency measures at about 100%.

Visual MINTEQ Simulation

Carbonate precipitations, including abiotic precipitation and biotic precipitation, in the test tube experiments, were reproduced using the Visual MINTEQ software package, investigating its speciation during the EICP process. Understanding the speciation of precipitations is considered of great necessity for revealing the mechanisms affecting Pb remediation. The reproduced carbonate precipitations, when subjected to urease at 3 g/L, 6 g/L, and 9 g/L, are shown in **Figure 4**. There are four precipitation speciations present, including $PbCl_2$, hydrocerrusite ($Pb_3(CO_3)_2(OH)_2$), lead carbonate ($PbCO_3$), and calcium carbonate ($CaCO_3$) (**Eqs 4**, **6**, **7**, **8**). $PbCl_2$ is categorized as abiotic precipitation since it is formed prior to introducing urease, while $Pb_3(CO_3)_2(OH)_2$, $PbCO_3$, and $CaCO_3$ are, therefore, classed as biotic precipitation. Furthermore, accompanied with the increase of the urease concentration, the precipitation speciation starts transforming. For example, $PbCl_2$ is transformed to $Pb_3(CO_3)_2(OH)_2$ in the first place when the urease concentration is increased from 3 g/L to 6 g/L (see **Figures 4A–C**). Subsequently, $Pb_3(CO_3)_2(OH)_2$ is transformed to $PbCO_3$ when the urease concentration is increased from 6 g/L to 9 g/L. Moreover, except $CaCO_3$ the concentrations of $PbCl_2$, $PbCO_3$, and $Pb_3(CO_3)_2(OH)_2$ are increased with the increase in the $Pb(NO_3)_2$ concentration. The simulated results indicate that the remediation efficiency against different urease concentrations performs very well and in excess of 99% on average, which is in line with the experimental results (see **Figures 1D**, **4D**).

$$Pb^{2+} + 2Cl^- \rightarrow PbCl_2 \downarrow, \tag{6}$$

$$3Pb^{2+} + 2CO_3^{2-} + 2OH^- \rightarrow Pb_3(CO_3)_2(OH)_2 \downarrow, \tag{7}$$

$$Pb^{2+} + CO_3^{2-} \rightarrow PbCO_3 \downarrow . \tag{8}$$

On the other hand, the reproduced carbonate precipitations when subjected to $CaCl_2$, $Ca(CH_3COO)_2$, and CaO are shown in **Figure 5**. Unlike the previous simulation, there are six speciations of carbonate precipitation, including $PbCl_2$, $Pb(OH)_2$, $Pb_3(CO_3)_2(OH)_2$, $PbCO_3$, $Ca(OH)_2$, and $CaCO_3$, when subjected to the effect of the calcium source (**Eqs 5–10**). $PbCl_2$, $Pb(OH)_2$, and $Ca(OH)_2$ are precipitated before catalyzing urea hydrolysis and are therefore classed as abiotic precipitations, while $CaCO_3$, $Pb_3(CO_3)_2(OH)_2$, and $PbCO_3$ are

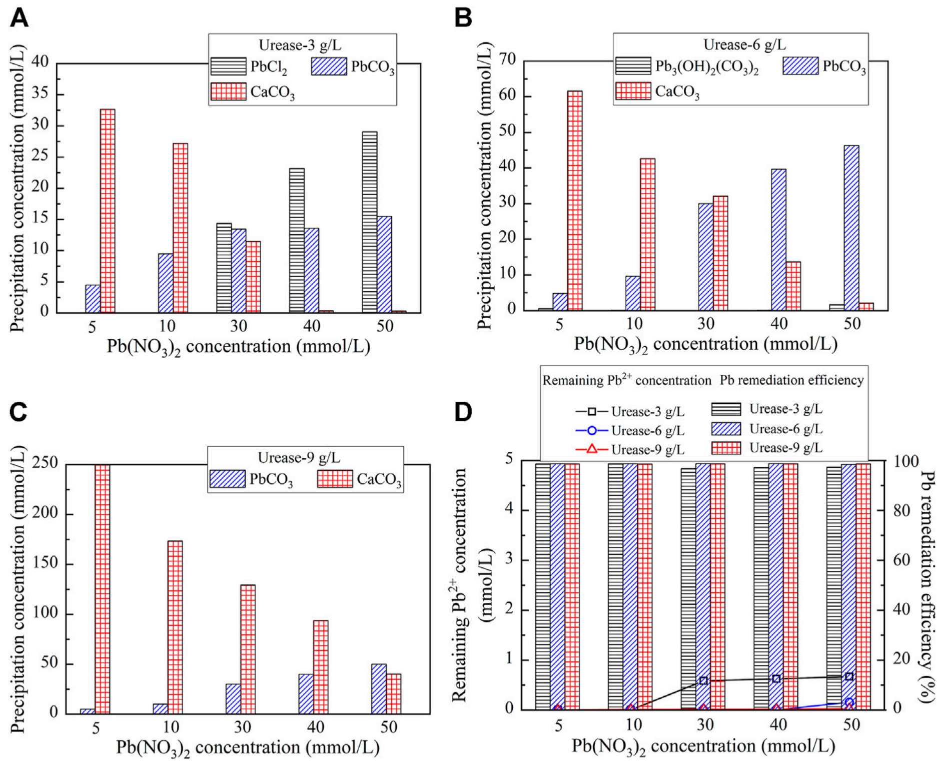

FIGURE 4 | Visual MINTEQ simulation under different urease concentrations: **(A)** 3 g/L; **(B)** 6 g/L; **(C)** 9 g/L; and **(D)** remaining Pb^{2+} concentration and remediation efficiency.

categorized as biotic precipitations. Furthermore, except $CaCO_3$ and $Ca(OH)_2$, the concentrations of $PbCl_2$, $Pb(OH)_2$, $Pb_3(CO_3)_2(OH)_2$, and $PbCO_3$ are increased with the increase in the concentration of $Pb(NO_3)_2$ (see **Figures 5A–C**). Last but not least, the remediation efficiency against different calcium sources surpasses 90% (see **Figure 5D**). There appears a discrepancy between the simulated results and the experimental ones (see **Figures 3B**, **5D**).

$$Pb + 2OH^- \rightarrow Pb(OH)_2 \downarrow, \tag{9}$$

$$CaO + H_2O \rightarrow Ca(OH)_2 \downarrow. \tag{10}$$

DISCUSSION

Effect of Urease Concentration

It can be seen from **Figure 1A** that the pH values for urease at 9 g/L are always higher than those for urease at 3 g/L, indicating a more comprehensive urea hydrolysis. The pH, when subjected to urease at 6 g/L and 9 g/L, respectively, shows a small change when the concentration of $Pb(NO_3)_2$ is increased from 5 mmol/L to 50 mmol/L. In contrast, when subjected to urease at 3 g/L, there appears a decrease in the pH of $Pb(NO_3)_2$ at 30 mmol/L. The lower the urease concentration, the more significant is the effect of Pb ions. A similar decrease can also be seen in **Figure 1B**; when subjected to urease at 9 g/L and 6 g/L, respectively, the NH_4^+ concentration generally decreases with the increase in the $Pb(NO_3)_2$ concentration. However, when subjected to urease at 3 g/L, there appears a NH_4^+ concentration drop in $Pb(NO_3)_2$ at 30 mmol/L. These results indicate that the effect of Pb ions can depress urea hydrolysis and becomes more significant when subjected to lower urease concentrations. In the present work, $Pb(NO_3)_2$ at or higher than 30 mmol/L starts depressing urea hydrolysis when subjected to urease at 3 g/L. Urease is essentially protein, and heavy metal ions can badly inactivate it by reacting with its sulfhydryl group (Shaw and Raval, 1961; Chung et al., 2020). Given that the NH_4^+ concentration reflects whether comprehensive urea hydrolysis is attained, enhancing our understanding of how the urease activity, when subjected to the effect of Pb ions, affects the production of NH_4^+ is considered of great necessity. For this reason, the relation of the urease activity and NH_4^+ concentration versus time is explored, as shown in **Supplementary Figure S2**. It can be observed that the degradation of the urease activity, when subjected to the Pb ions, is not instantaneous (Yuan et al., 2020) and can be further divided into three phases, including the rapid degradation phase, gentle degradation phase, and limited degradation phase, according to the change of the NH_4^+ concentration. During the rapid degradation phase, the Pb ions cause the urease activity to decrease very quickly, while the NH_4^+ concentration is increased over time, indicating that urease has not been inactivated yet. The urease activity decreases progressively during the gentle degradation phase where the increase of the NH_4^+ concentration due to the reduced urease activity is not as significant as before. In the limited degradation phase, the NH_4^+

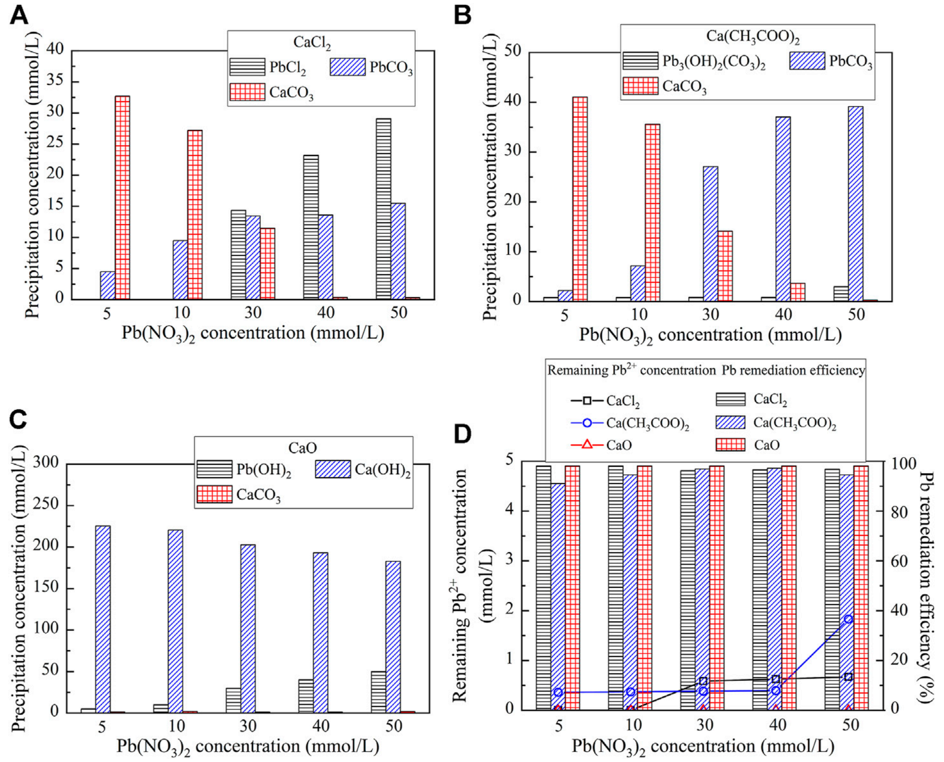

FIGURE 5 | Visual MINTEQ simulation under different calcium sources: **(A)** CaCl$_2$; **(B)** Ca(CH$_3$COO)$_2$; **(C)** CaO; and **(D)** remaining Pb^{2+} concentration and remediation efficiency.

concentration shows a small change, indicating that urease has already been inactivated.

It is well acknowledged that the degradation of the urease activity is accompanied by carbonate precipitation, and the speciation of carbonate precipitation determines whether a fairly good Pb remediation is attained. The following content aims to address how the speciation of carbonate precipitation affects the Pb remediation efficiency. The simulated results indicate that the speciation of carbonate precipitation, when subjected to the urease concentration at 9 g/L, includes PbCO$_3$ and CaCO$_3$, and they are classed as biotic precipitations. The biotic precipitations are relatively stable compared to the abiotic ones, according to their solubility product (termed K$_{sp}$ hereafter). Their transformation is, therefore, not going to happen (Jiang et al., 2019; Xue et al., 2022). Provided that higher urease concentrations ensure the availability of CO$_3^{2-}$, a fairly satisfactory Pb remediation can be expected. In contrast, the speciation of carbonate precipitation under the urease concentration at 3 g/L comprises PbCl$_2$, CaCO$_3$, and PbCO$_3$. Two of them (CaCO$_3$ and PbCO$_3$) are categorized as biotic precipitations and PbCl$_2$ as an abiotic one. The Pb remediation efficiencies under 3 g/L and 9 g/L urease concentrations are approximately 100%, although the associated precipitation speciation differs from each other. Given that K$_{sp}$ (PbCl$_2$) being 1.6×10^{-6} is greater than K$_{sp}$ (PbCO$_3$) being 7.4×10^{-14}, PbCl$_2$ is more likely to be dissolved and converted to other chemical substances compared with PbCO$_3$. Thus, PbCO$_3$ is deemed as a desirable precipitation compound rather than PbCl$_2$. To summarize, the effect of Pb ions depresses urea hydrolysis and becomes more significant when subjected to lower urease concentrations. Higher urease concentrations ensure the availability of CO$_3^{2-}$, contributing to a formation of a relatively stable biotic precipitation.

Effect of Calcium Source

As the calcium source can affect the speciation of carbonate precipitation, measurements of pH and NH$_4^+$ concentrations can benefit us in enhancing our understanding of the effect of the calcium source on Pb remediation (Jiang et al., 2019). For a given Pb(NO$_3$)$_2$ concentration, the pH is measured the highest when subjected to CaO, followed by CaCl$_2$ (see **Figures 2A,C**), while the pH is measured the lowest when subjected to Ca(CH$_3$COO)$_2$ (see **Figure 2B**). The highest pH derived from CaO appears to indicate the comprehensive urea hydrolysis. In fact, while using CaO as the calcium source, the CaO reacts with H$_2$O to form Ca(OH)$_2$ toward elevating the value of pH. This is in line with the measurements of pH. The pH reaches a value as high as 12 (see **Figure 2C**). Notwithstanding this fact, such a high pH depresses the urease activity, resulting in a reduction of the NH$_4^+$ concentration (Mobley and Hausinger, 1989; Neupane et al., 2013; and Almajed et al., 2018) (see **Figure 2D**). The measured results of the NH$_4^+$ concentration also confirm this statement. On the other hand, the NH$_4^+$ concentration for a given Pb(NO$_3$)$_2$ concentration is measured the highest under

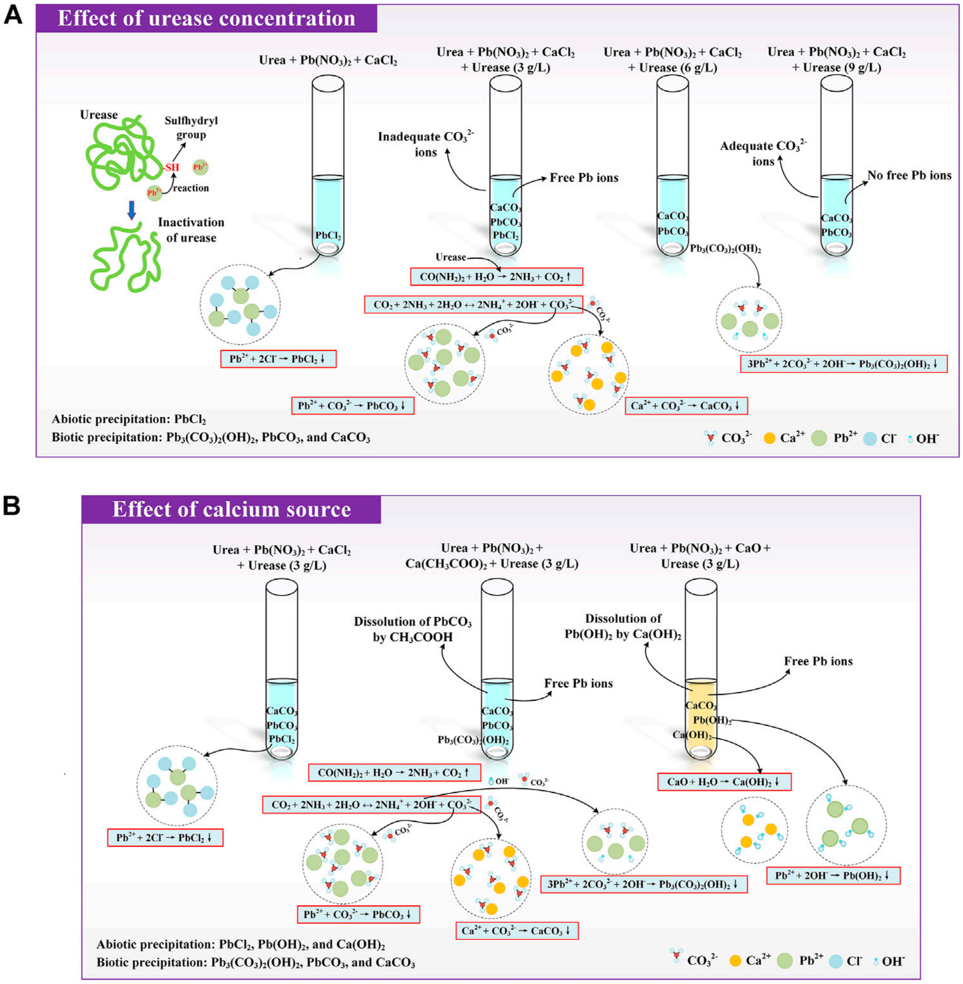

FIGURE 6 | (A) Schematic illustration of the effect of urease concentration on Pb remediation and **(B)** Schematic illustration of the effect of the calcium source on Pb remediation.

$Ca(CH_3COO)_2$, followed by $CaCl_2$. As a result, the calcium source depresses the urease activity by influencing the surrounding pH, resulting in a reduction of the NH_4^+ concentration.

The speciation of carbonate precipitation is also explored here to extend the interpretation of the experimental and simulated results. The simulated results indicate that the speciation of the carbonate precipitation, when subjected to the calcium source of CaO, includes $Pb(OH)_2$, $Ca(OH)_2$, and $CaCO_3$ where the former two are classed as abiotic precipitations. $Ca(OH)_2$ is formed before $Pb(OH)_2$ due to the addition sequence of calcium sources. Given that K_{sp} ($Ca(OH)_2$) being 5.5×10^{-6} is greater than K_{sp} ($Pb(OH)_2$) being 1.2×10^{-15}, $Ca(OH)_2$ tends to transform to $Pb(OH)_2$. However, $Pb(OH)_2$ is deemed soluble when exposed to alkaline environments (Edwards et al., 1992; Baltpurvins et al., 1996; Vítková et al., 2009; and Wang et al., 2022). When $Pb(OH)_2$ is just formed following the aforesaid transformation, and it is also on the way to dissolve, thereby releasing the Pb ions into the solution. This also means a degradation of the Pb remediation. Furthermore, the speciation of carbonate precipitation under the calcium source of $Ca(CH_3COO)_2$ comprises $Pb_3(CO_3)_2(OH)_2$, $PbCO_3$, and $CaCO_3$, and they are classed as biotic precipitations. Under the calcium source of $CaCl_2$, two of them ($CaCO_3$ and $PbCO_3$) are categorized as biotic precipitations and $PbCl_2$ as an abiotic one. The abiotic precipitation compensates for the deficiency of carbonate precipitation caused by the lack of CO_3^{2-}. Therefore, the formation of biotic and abiotic precipitation results in the highest Pb remediation efficiency although the NH_4^+ concentration is not the highest under the calcium source of $CaCl_2$.

Generally, the higher the precipitation mass, the higher is the remediation efficiency. However, this sometimes causes a misleading interference while assessing the Pb remediation efficiency. In the present work, there appears a discrepancy of Pb remediation between the experimental and simulated results (see **Figures 3B, 5D**). Despite this fact, the highest precipitation mass against different Pb(NO3)2 concentrations is derived using CaO, and the highest remediation efficiency is, however, derived using $CaCl_2$. In light of

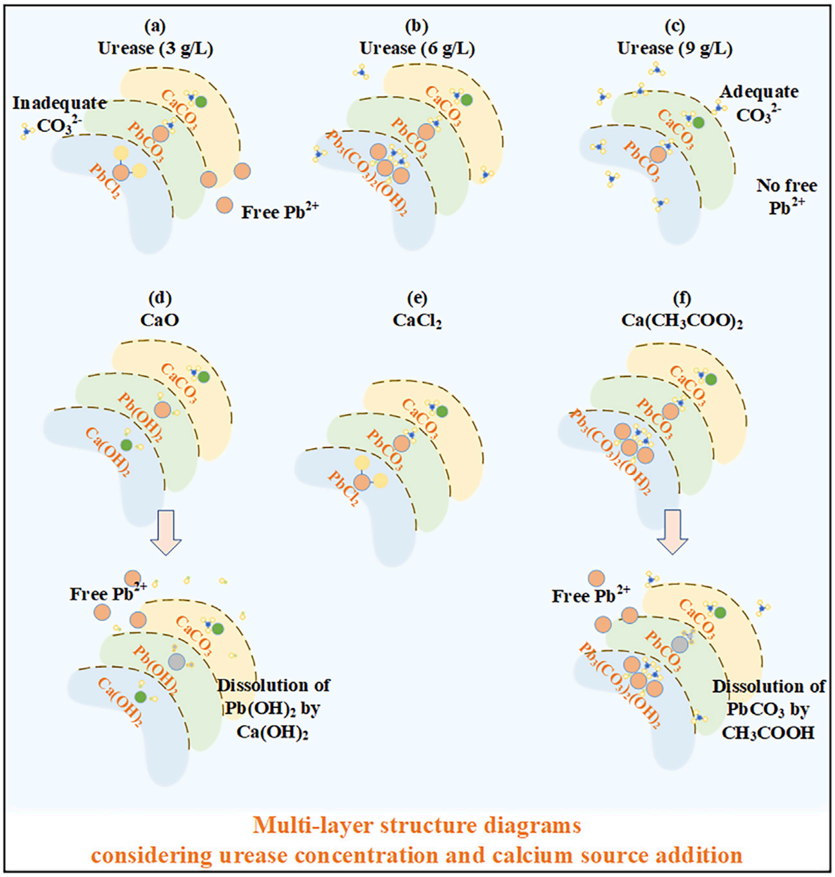

FIGURE 7 | Schematic illustration of the multi-layer structure of carbonate precipitation: **(A)** urease at 3 g/L; **(B)** urease at 6 g/L; **(C)** urease at 9 g/L; **(D)** CaO; **(E)** $CaCl_2$; and **(F)** $Ca(CH_3COO)_2$.

this, the Pb remediation is not only determined by the precipitation mass but also by the speciation of precipitation. As discussed, the dissolution of $Pb(OH)_2$, while using CaO, releases free Pb ions and subsequently degrades Pb remediation, which has been neglected in the simulation. This is considered as the main cause leading to the discrepancy between the experimental and simulated results.

Mechanisms Affecting Lead Remediation

The change of the NH_4^+ concentration confirms that the Pb ions notably depress the urease activity, and the effect of the Pb ions becomes more significant when subjected to lower urease concentrations (see **Figure 6A**). In these circumstances, the availability of CO_3^{2-} cannot be consistently assured during the EICP process, thereby degrading Pb remediation. These results indicate that higher urease concentrations not only counterbalance the effect of the Pb ions but also assure the availability of CO_3^{2-} toward securing a formation of the relatively stable biotic precipitation. On the other hand, the highest pH is derived using CaO, most likely because of the elevation of pH by $Ca(OH)_2$. The urease activity is depressed accordingly, and when exposed to alkaline environments, the dissolution of $Pb(OH)_2$ releases Pb ions to degrade Pb remediation (see **Figure 6B**). The highest Pb remediation is attained using $CaCl_2$ where the pH is measured in the second place. In short, a combination of higher urease concentrations and an appropriate calcium source may be used to prevent the degradation of Pb remediation.

In addition to the effects of the urease concentration and calcium source, the precipitation mass also has implications on Pb remediation. The precipitation mass under the urease concentration at 9 g/L is higher than that under the urease concentration at 3 g/L, making the discrepancy in Pb remediation efficiency negligible. Meanwhile, the highest precipitation mass against different calcium sources is attained using CaO, and the highest Pb remediation is, however, attained using $CaCl_2$. These results confirm that Pb remediation is not only determined by the precipitation mass but also by other influencing factors (e.g., speciation and sequence of carbonate precipitation). When subjected to the urease concentration at 3 g/L, $PbCl_2$ first precipitates to form the inner layer of a multi-layer structure, followed by $PbCO_3$ and $CaCO_3$ to form its outer layer (see **Figures 7A–C**). The multi-layer structure prevents the migration of Pb ions, although a small number of free Pb ions is released as a result of the inadequacy of CO_3^{2-}. In contrast, the multi-layer structure of carbonate precipitation under urease at 9 g/L can be recognized as $PbCO_3$ and $CaCO_3$ forming the inner and outer layers, respectively, thereby preventing the migration of Pb ions. On the other hand, $Pb_3(CO_3)_2(OH)_2$, when subjected to $Ca(CH_3COO)_2$, precipitates in the first place, followed by $PbCO_3$ and $CaCO_3$ (see **Figures 7D–F**). When subjected to CaO, the carbonate precipitation sequence can be sorted as $Ca(OH)_2$, $Pb(OH)_2$, and $CaCO_3$. However, $Pb(OH)_2$ is dissolved in alkaline conditions resulting from $Ca(OH)_2$, and Pb ions are released, degrading Pb remediation (Edwards et al., 1992; Baltpurvins et al., 1996; Vítková et al., 2009). Moreover, $PbCl_2$ under $CaCl_2$ first precipitates, followed by $PbCO_3$ and $CaCO_3$, meaning that a multi-layer structure of carbonate precipitation is developed, and $PbCl_2$ forms the inner layer, covered by the two outer layers, including $PbCO_3$ and $CaCO_3$. The multi-layer structure of the carbonate precipitation encapsulates the Pb ions and causes some difficulty for the Pb ions to migrate, stabilizing the Pb ions and preventing the degradation of Pb remediation. The multi-layer structure of carbonate precipitation, when subjected to CaO, would have been more effective in stabilizing the Pb ions if the dissolution of $Pb(OH)_2$ had not happened.

On the whole, Pb ions depress the urease activity, and the effect of Pb ions turns into a more pronounced contributor when subjected to lower urease concentrations. Higher urease concentrations can consistently assure the availability of CO_3^{2-} during the EICP process. The use of a calcium source can affect the speciation of carbonate precipitation. In some cases, an inappropriate calcium source can cause difficulty in developing the multi-layer structure of carbonate precipitation, thereby degrading Pb remediation. The use of higher urease concentrations and an appropriate calcium source can prevent the degradation of Pb remediation. Furthermore, Pb remediation is not only determined by the precipitation mass but also by other influencing factors. The precipitation sequence plays a role in the formation of the multi-layer structure of carbonate precipitation. The multi-layer structure capsulizes Pb ions and, therefore, prevents their migration, securing the Pb remediation efficiency. The robustness of the multi-layer structure of carbonate precipitation cannot be quantitatively assessed by a micro-structural analysis but by the speciation analysis of Pb^{2+}. Details about the results of the micro-structural and speciation analyses are not within the scope of the present work and would be discussed in another article.

CONCLUSION

This article has investigated the effects of the urease concentration and a calcium source on Pb remediation. The speciation and sequence of carbonate precipitation have been explored to highlight the mechanisms leading to the degradation of Pb remediation. Based on the results and discussion, some main conclusions can be drawn as follows:

1) The NH_4^+ concentration presents good correspondence with the urease concentration. As indicated by the NH_4^+ concentration, the Pb ions depress the urease activity, and the effect of Pb ions becomes more significant when provided with lower urease concentrations. Higher urease concentrations can assure the availability of CO_3^{2-} during the EICP process toward benefiting carbonate precipitation.
2) The calcium source, in fact, determines the speciation of carbonate precipitation and subsequently the Pb remediation efficiency. The Pb remediation efficiency is not only determined by the precipitation mass but also by the other influencing factors (e.g., precipitation sequence). The dissolution of $Pb(OH)_2$, when subjected to CaO, has been neglected in the Visual MINTEQ simulation, causing a discrepancy of Pb remediation between the experimental and simulated results. In the present study, the highest Pb remediation efficiency is attained using $CaCl_2$. The abiotic precipitation compensates for the deficiency of carbonate precipitation caused by the lack of CO_3^{2-}.
3) The use of CaO results in the dissolution of $Pb(OH)_2$ and, therefore, releases Pb ions, causing some difficulty in forming the multi-layer structure of carbonate precipitation and degrading Pb remediation. Given that $PbCl_2$ is precipitated first, followed by $PbCO_3$ and $CaCO_3$, when subjected to $CaCl_2$, the multi-layer structure of carbonate precipitation capsulizes the Pb ions and prevents their migration, securing Pb remediation. The present work highlights the exciting potential of applying the EICP technology to Pb ion removal. Further work of stabilizing Pb ions in the contaminated sites by the EICP technology is ongoing and would be discussed in another article.

DATA AVAILABILITY STATEMENT

The original contributions presented in the study are included in the article/**Supplementary Material**, further inquiries can be directed to the corresponding author.

AUTHOR CONTRIBUTIONS

LW: data curation, formal analysis, validation, software, and writing—original draft. W-CC: conceptualization, methodology, writing—review and editing, supervision, and funding acquisition. Z-FX: writing—review and editing. WH: writing—review and editing.

FUNDING

This study is based upon work supported by the Shaanxi Educational Department under Grant No. 2020TD-005 through the innovative ability support scheme.

SUPPLEMENTARY MATERIAL

The Supplementary Material for this article can be found online at: https://www.frontiersin.org/articles/10.3389/fchem.2022.892090/full#supplementary-material

REFERENCES

Achal, V., Mukerjee, A., and Sudhakara Reddy, M. (2013). Biogenic Treatment Improves the Durability and Remediates the Cracks of concrete Structures. *Construction Building Mater.* 48, 1–5. doi:10.1016/j.conbuildmat.2013.06.061

Achal, V., Pan, X., Fu, Q., and Zhang, D. (2012). Biomineralization Based Remediation of As(III) Contaminated Soil by *Sporosarcina Ginsengisoli*. *J. Hazard. Mater.* 201, 178–184. doi:10.1016/j.jhazmat.2011.11.067

Ahenkorah, I., Rahman, M. M., Karim, M. R., and Beecham, S. (2021a). Optimisation of Chemical Constituents on Enzyme-Induced Carbonate Precipitation in Test-Tube and Soil. *Geotechnical Res.* 5 (3), 1–19. doi:10.1680/jgere.21.00006

Ahenkorah, I., Rahman, M. M., Karim, M. R., Beecham, S., and Saint, C. (2021b). A Review of Enzyme Induced Carbonate Precipitation (EICP): The Role of Enzyme Kinetics. *Sustain. Chem.* 2, 92–114. doi:10.3390/suschem2010007

Almajed, A., Khodadadi Tirkolaei, H., and Kavazanjian, E. (2018). Baseline Investigation on Enzyme-Induced Calcium Carbonate Precipitation. *J. Geotech. Geoenviron. Eng.* 144 (11), 04018081. doi:10.1061/(asce)gt.1943-5606.0001973

An, Q., Deng, S., Xu, J., Nan, H., Li, Z., and Song, J. L. (2019). Simultaneous Reduction of Nitrate and Cr(VI) by *Pseudomonas aeruginosa* Strain G12 in Wastewater. *Ecotoxicol Environ. Saf.* 191, 110001. doi:10.1016/j.ecoenv.2019.110001

Bai, B., Long, F., Rao, D. Y., and Xu, T. (2017). The Effect of Temperature on the Seepage Transport of Suspended Prticles in a Porous Medium. *Hydrol Process* 31 2, 382–393. doi:10.1002/hyp.11034

Bai, B., Nie, Q. K., Zhang, Y. K., Wang, X. L., and Xu, W. (2021). Cotransport of Heavy Metals and SiO2 Particles at Different Temperatures by Seepage. *J. Hydrol.* 597, 125771. doi:10.1016/j.jhydrol.2020.125771

Bai, X. D., Cheng, W. C., and Li, G. (2021). A Comparative Study of Different Machine Learning Algorithms in Predicting EPB Shield Behavior: A Case Study at Xi'an Metro, China. *Acta geotechnica* 16 12, 4061–4080. doi:10.1007/s11440-021-01383-7

Baltpurvins, K. A., Burns, R. C., Lawrance, G. A., and Stuart, A. D. (1996). Use of the Solubility Domain Approach for the Modeling of the Hydroxide Precipitation of Heavy Metals from Wastewater. *Environ. Sci. Technol.* 30, 1493–1499. doi:10.1021/es950421u

Chang, J., Deng, S., Liang, Y., and Chen, J. (2019). Cr(VI) Removal Performance from Aqueous Solution by *Pseudomonas* Sp. Strain DC-B3 Isolated from Mine Soil: Characterization of Both Cr(VI) Bioreduction and Total Cr Biosorption Processes. *Environ. Sci. Pollut. Res.* 26 (27), 28135–28145. doi:10.1007/s11356-019-06017-w

Chen, L., Beiyuan, J., Hu, W., Zhang, Z., Duan, C., Cui, Q., et al. (2022a). Phytoremediation of Potentially Toxic Elements (PTEs) Contaminated Soils Using Alfalfa (Medicago Sativa L.): A Comprehensive Review. *Chemosphere* 293, 133577. doi:10.1016/j.chemosphere.2022.133577

Chen, L., Wang, J., Beiyuan, J., Guo, X., Wu, H., and Fang, L. (2022b). Environmental and Health Risk Assessment of Potentially Toxic Trace Elements in Soils Near Uranium (U) Mines: A Global Meta-Analysis. *Sci. Total Environ.* 816, 151556. doi:10.1016/j.scitotenv.2021.151556

Chen, Y., Gao, Y., Ng, C. W. W., and Guo, H. (2021). Bio-improved Hydraulic Properties of Sand Treated by Soybean Urease Induced Carbonate Precipitation and its Application Part 1: Water Retention Ability. *Transportation Geotechnics* 27, 100489. doi:10.1016/j.trgeo.2020.100489

Cheng, W. C., Duan, Z., Xue, Z. F., and Wang, L. (2021). Sandbox Modelling of Interactions of Landslide Deposit with Terrace Sediments Aided by Field Observation. *Bulletin of Engineering Geology and the Environment* 80, 100489. doi:10.1007/s10064-021-02144-2

Chung, H., Kim, S. H., and Nam, K. (2020). Inhibition of Urea Hydrolysis by Free Cu Concentration of Soil Solution in Microbially Induced Calcium Carbonate Precipitation. *Sci. Total Environ.* 740, 3711–3731. doi:10.1007/s10064-021-02144-2

Cui, M.-J., Lai, H.-J., Hoang, T., and Chu, J. (2021). One-phase-low-pH Enzyme Induced Carbonate Precipitation (EICP) Method for Soil Improvement. *Acta Geotech.* 16, 481–489. doi:10.1007/s11440-020-01043-2

Dhami, N. K., Reddy, M. S., and Mukherjee, A. (2013). Biomineralization of Calcium Carbonates and Their Engineered Applications: a Review. *Front. Microbiol.* 4, 314. doi:10.3389/fmicb.2013.00314

Duan, Q., Lee, J., Liu, Y., Chen, H., and Hu, H. (2016). Distribution of Heavy Metal Pollution in Surface Soil Samples in China: A Graphical Review. *Bull. Environ. Contam. Toxicol.* 97 (3), 303–309. doi:10.1007/s00128-016-1857-9

Duan, Z., Cheng, W. C., Peng, J. B., and Tang, H. (2021). Interactions of Landslide Deposit with Terrace Sediments: Perspectives from Velocity of Deposit Movement and Apparent Friction Angle. *Engineering Geology* 280, 105913. doi:10.1016/j.enggeo.2020.105913

Edwards, R., Gillard, R. D., Williams, P. A., and Pollard, A. M. (1992). Studies of Secondary mineral Formation in the PbO-H2o-HC1 System. *Mineral. Mag.* 56, 53–65. doi:10.1180/minmag.1992.056.382.07

Fisher, K. A., Yarwood, S. A., and James, B. R. (2017). Soil Urease Activity and Bacterial ureC Gene Copy Numbers: Effect of pH. *Geoderma* 285, 1–8. doi:10.1016/j.geoderma.2016.09.012

Fujita, Y., Taylor, J. L., Wendt, L. M., Reed, D. W., and Smith, R. W. (2010). Evaluating the Potential of Native Ureolytic Microbes to Remediate a 90Sr Contaminated Environment. *Environ. Sci. Technol.* 44, 7652–7658. doi:10.1021/es101752p

Gat, D., Ronen, Z., and Tsesarsky, M. (2017). Long-term Sustainability of Microbial-Induced CaCO3 Precipitation in Aqueous media. *Chemosphere* 184, 524–531. doi:10.1016/j.chemosphere.2017.06.015

Hamdan, N. E. K., and Kavazanjian, E. (2016). Enzyme-induced Carbonate mineral Precipitation for Fugitive Dust Control. *Géotechnique* 66 (7), 546–555. doi:10.1680/jgeot.15.p.168

Hoang, T., Alleman, J., Cetin, B., Ikuma, K., and Choi, S.-G. (2019). Sand and Silty-Sand Soil Stabilization Using Bacterial Enzyme-Induced Calcite Precipitation (BEICP). *Can. Geotech. J.* 56, 808–822. doi:10.1139/cgj-2018-0191

Hu, W., Cheng, W.-C., Wen, S., and Yuan, K. (2021). Revealing the Enhancement and Degradation Mechanisms Affecting the Performance of Carbonate Precipitation in EICP Process. *Front. Bioeng. Biotechnol.* 9, 750258. doi:10.3389/fbioe.2021.750258

Hu, X. F., Huang, X. R., Zhao, H. H., Liu, F. H., Wang, L., Zhao, X., et al. (2020). Possibility of Using Modified Fly Ash and Organic Fertilizers for Remediation of Heavy-Metal-Contaminated Soils. *J. Clean. Prod.* 284 (7), 124713. doi:10.1016/j.jclepro.2020.124713

Hu, W., Cheng, W. C., Wen, S., and Mizanur Rahman, N. (2021). Effects of Chemical Contamination on Microscale Structural Characteristics of Intact Loess and Resultant Macroscale Mechanical Properties. *Catena* 203, 105361. doi:10.1016/j.catena.2021.105361

Hu, W., Cheng, W. C., Wang, L., and Xue, Z. F. (2022). Micro-Structural Characteristics Deterioration of Intact Loess Under Acid and Saline Solutions and Resultant Macro-Mechanical Properties. *Soil and Tillage Research* 220, 105382. doi:10.1016/j.still.2022.105382

Jiang, N.-J., Liu, R., Du, Y.-J., and Bi, Y.-Z. (2019). Microbial Induced Carbonate Precipitation for Immobilizing Pb Contaminants: Toxic Effects on Bacterial Activity and Immobilization Efficiency. *Sci. Total Environ.* 672, 722–731. doi:10.1016/j.scitotenv.2019.03.294

Jiang, N. J., Wang, Y. J., Chu, J., Kawasaki, S., Tang, C. S., Cheng, L., et al. (2021). Bio-mediated Soil Improvement: An Introspection into Processes, Materials, Characterization and Applications. *Soil Use Manage.* 38, 12736. doi:10.1111/sum.12736

Kang, C.-H., and So, J.-S. (2016). Heavy Metal and Antibiotic Resistance of Ureolytic Bacteria and Their Immobilization of Heavy Metals. *Ecol. Eng.* 97, 304–312. doi:10.1016/j.ecoleng.2016.10.016

Keykha, H. A., Asadi, A., Huat, B. B. K., and Kawasaki, S. (2018). Laboratory Conditions Formaximal Calcium Carbonate Precipitation Induced by Sporosarcina Pasteurii and Sporosarcina Aquimarina Bacteria. *Environ. Geotechnics* 6 (8), 1–20. doi:10.1680/jenge.16.00009

Kim, S. O., Moon, S. H., and Kim, K. W. (2001). Removal of Heavy Metals from Soils Using Enhanced Electrokinetic Soil Processing. *Water Air Soil Pollut.* 125 (1), 259–272. doi:10.1023/a:1005283001877

Kumar, V., and Dwivedi, S. K. (2019). Hexavalent Chromium Stress Response, Reduction Capability and Bioremediation Potential of Trichoderma Sp. Isolated from Electroplating Wastewater. *Ecotoxicology Environ. Saf.* 185, 109734. doi:10.1016/j.ecoenv.2019.109734

Li, M., Fu, Q.-L., Zhang, Q., Achal, V., and Kawasaki, S. (2015). Bio-grout Based on Microbially Induced Sand Solidification by Means of Asparaginase Activity. *Sci. Rep.* 5, 16128. doi:10.1038/srep16128

Liu, B., Xie, Y.-H., Tang, C.-S., Pan, X.-H., Jiang, N.-J., Singh, D. N., et al. (2021). Bio-mediated Method for Improving Surface Erosion Resistance of Clayey Soils. *Eng. Geology*. 293, 106295. doi:10.1016/j.enggeo.2021.106295

Meng, H., Shu, S., Gao, Y., Yan, B., and He, J. (2021). Multiple-phase Enzyme-Induced Carbonate Precipitation (EICP) Method for Soil Improvement. *Eng. Geology*. 294, 106374. doi:10.1016/j.enggeo.2021.106374

Mobley, H. L., and Hausinger, R. P. (1989). Microbial Ureases: Significance, Regulation, and Molecular Characterization. *Microbiol. Rev.* 53 (1), 85–108. doi:10.1128/mr.53.1.85-108.1989

Moghal, A. A. B., Lateef, M. A., Mohammed, S. A. S., Ahmad, M., Usman, A. R. A., and Almajed, A. (2020b). Heavy Metal Immobilization Studies and Enhancement in Geotechnical Properties of Cohesive Soils by EICP Technique. *Appl. Sci.* 10 (7568), app10217568. doi:10.3390/app10217568

Moghal, A. A. B., Lateef, M. A., Mohammed, S. A. S., Lemboye, K., Chittoori, B. C. S., and Almajed, A. (2020a). Efficacy of Enzymatically Induced Calcium Carbonate Precipitation in the Retention of Heavy Metal Ions. *Sustainability* 12 (7019), su12177019. doi:10.3390/su12177019

Mohan, S. V., Kisa, T., Ohkuma, T., Kanaly, R. A., and Shimizu, Y. (2006). Bioremediation Technologies for Treatment of PAH-Contaminated Soil and Strategies to Enhance Process Efficiency. *Rev. Environ. Sci. Biotechnol.* 5 (4), 347–374. doi:10.1007/s11157-006-0004-1

Mugwar, A. J., and Harbottle, M. J. (2016). Toxicity Effects on Metal Sequestration by Microbially-Induced Carbonate Precipitation. *J. Hazard. Mater.* 314, 237–248. doi:10.1016/j.jhazmat.2016.04.039

Nafisi, A., Safavizadeh, S., and Montoya, B. M. (2019). Influence of Microbe and Enzyme-Induced Treatments on Cemented Sand Shear Response. *J. Geotech. Geoenviron. Eng* 145 (9), 06019008. doi:10.1061/(asce)gt.1943-5606.0002111

Nam, I.-H., Roh, S.-B., Park, M.-J., Chon, C.-M., Kim, J.-G., Jeong, S.-W., et al. (2016). Immobilization of Heavy Metal Contaminated Mine Wastes Using Canavalia Ensiformis Extract. *Catena* 136, 53–58. doi:10.1016/j.catena.2015.07.019

Neupane, D., Yasuhara, H., Kinoshita, N., and Unno, T. (2013). Applicability of Enzymatic Calcium Carbonate Precipitation as a Soil-Strengthening Technique. *J. Geotech. Geoenviron. Eng.* 139 (12), 2201–2211. doi:10.1061/(asce)gt.1943-5606.0000959

Phillips, A. J., Gerlach, R., Lauchnor, E., Mitchell, A. C., Cunningham, A. B., and Spangler, L. (2013). Engineered Applications of Ureolytic Biomineralization: a Review. *Biofouling* 29, 715–733. doi:10.1080/08927014.2013.796550

Putra, H., Yasuhara, H., Kinoshita, N., Neupane, D., and Lu, C. W. (2016). Effect of Magnesium as Substitute Material in Enzyme-Mediated Calcite Precipitation for Soil-Improvement Technique. *Front. Bioeng. Biotechnol.* 4, 37–38. doi:10.3389/fbioe.2016.00037

Qian, X., Fang, C., Huang, M., and Achal, V. (2017). Characterization of Fungal-Mediated Carbonate Precipitation in the Biomineralization of Chromate and lead from an Aqueous Solution and Soil. *J. Clean. Prod.* 164 (15), 198–208. doi:10.1016/j.jclepro.2017.06.195

Rahman, M. M., Hora, R. N., Ahenkorah, I., Beecham, S., Karim, M. R., and Iqbal, A. (2020). State-of-the-art Review of Microbial-Induced Calcite Precipitation and its Sustainability in Engineering Applications. *Sustainability* 12 (6281), su12156281. doi:10.3390/su12156281

Shashank, B. S., Sharma, S., Sowmya, S., Latha, R. A., Meenu, P. S., and Singh, D. N. (2016). State-of-the-art on Geotechnical Engineering Perspective on Bio-Mediated Processes. *Environ. Earth Sci.* 75 (3), 270. doi:10.1007/s12665-015-5071-6

Shaw, W. H. R., and Raval, D. N. (1961). The Inhibition of Urease by Metal Ions at pH 8.9. *J. Am. Chem. Soc.* 83 (15), 3184–3187. doi:10.1021/ja01476a004

Sun, X., Miao, L., Wang, H., Yuan, J., and Fan, G. (2021). Enhanced Rainfall Erosion Durability of Enzymatically Induced Carbonate Precipitation for Dust Control. *Sci. Total Environ.* 791, 148369. doi:10.1016/j.scitotenv.2021.148369

Van Paassen, L. A. (2011). *Bio-mediated Ground Improvement: From Laboratory experiment to Pilot Applications*. Dallas, Texas, United States: ASCE, 4099–4108.

Vítková, M., Ettler, V., Sebek, O., Mihaljeviõc, M., Grygar, T., and Rohovec, J. (2009). The pH-dependent Leaching of Inorganic Contaminants from Secondary lead Smelter Fly Ash. *J. Hazard. Mater.* 167, 427–433. doi:10.1016/j.jhazmat.2008.12.136

Wang, L., Cheng, W.-C., and Xue, Z.-F. (2022). The Effect of Calcium Source on Pb and Cu Remediation Using Enzyme-Induced Carbonate Precipitation. *Front. Bioeng. Biotechnol.* 10, 849631. doi:10.3389/fbioe.2022.849631

Wang, L., Cheng, W. C., and Xue, Z. F. (2022). Investigating microscale structural characteristics and resultant macroscale mechanical properties of loess exposed to alkaline and saline environments. *B Eng. Geol environ.* 81, 146. doi:10.1007/s10064-022-02640-z

Wei, W., Shao, Z. S., Qiao, R. J., Chen, W. W., Zhang, P. J., and Cheng, J. X. (2021). Workability and Mechanical Properties of Microwave Heating for Recovering High Quality Aggregate From Concrete. *Construction and Building Materials* 276, 122237. doi:10.1016/j.conbuildmat.2020.122237

Wu, M., Hu, X., Zhang, Q., Zhao, Y., Sun, J., Cheng, W., et al. (2020). Preparation and Performance Evaluation of Environment-Friendly Biological Dust Suppressant. *J. Clean. Prod.* 273, 123162. doi:10.1016/j.jclepro.2020.123162

Xue, Z.-F., Cheng, W.-C., Wang, L., and Hu, W. (2022). Effects of Bacterial Inoculation and Calcium Source on Microbial-Induced Carbonate Precipitation for lead Remediation. *J. Hazard. Mater.* 426, 128090. doi:10.1016/j.jhazmat.2021.128090

Xue, Z. F., Cheng, W. C., Wang, L., and Song, G. Y. (2021). Improvement of the Shearing Behaviour of Loess Using Recycled Straw Fiber Reinforcement. *KSCE J. Civ. Eng.* 25 9, 3319–3335. doi:10.1007/s12205-021-2263-3

Yang, Y. Y., Wu, H. L., and Du, Y. J. (2014). Strength and Leaching Characteristics of Heavy Metal Contaminated Soils Solidified by Cement. *J. Residuals Sci. Techn.* 11 (3), 71–98.

Yuan, H., Ren, G., Liu, K., Zheng, W., and Zhao, Z. (2020). Experimental Study of EICP Combined with Organic Materials for silt Improvement in the Yellow River Flood Area. *Appl. Sci.* 10, 7678. doi:10.3390/app10217678

Yuan, Y., Shao, Z. S., Qiao, R. J., Fei, X. S., Cheng, J. X., and Wei, W. (2021). Fracture Behavior of Concrete Coarse Aggregates Under Microwave Irradiation Influenced by Mineral Components. *Construction and Building Materials* 286, 122944. doi:10.1016/j.conbuildmat.2021.122944

Zhu, Y., Ma, N., Jin, W., Wu, S., and Sun, C. (2017). Genomic and Transcriptomic Insights into Calcium Carbonate Biomineralization by marine Actinobacterium Brevibacterium Linens BS258. *Front. Microbiol.* 8, 602–614. doi:10.3389/fmicb.2017.00602

Conflict of Interest: The authors declare that the research was conducted in the absence of any commercial or financial relationships that could be construed as a potential conflict of interest.